Transmittance photoplethysmography with near-infrared laser diodes in intra-peritoneal organs

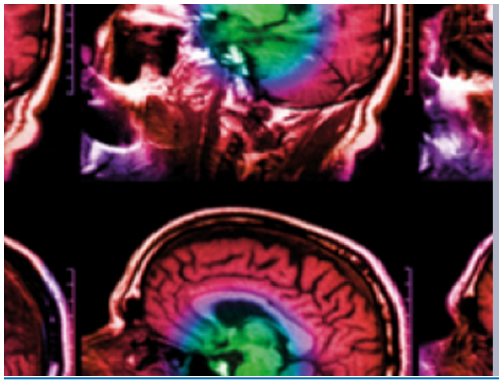

INSTITUTE OF PHYSICS PUBLISHING PHYSIOLOGICAL MEASUREMENT

Physiol. Meas. **27** (2006) 1033–1045 doi:10.1088/0967-3334/27/10/009

Transmittance photoplethysmography with near-infrared laser diodes in intra-peritoneal organs

S M López-Silva[1], J P Silveira[2], M L Dotor[2], R Giannetti[3], D Golmayo[4] and L Herrera[5]

[1] IUMA, Universidad de Las Palmas de Gran Canaria, Las Palmas 35017, Spain
[2] Instituto de Microelectrónica de Madrid, CNM-CSIC, Madrid 28760, Spain
[3] DEA, Universidad Pontificia Comillas de Madrid, Madrid 28015, Spain
[4] Instituto de Ciencia de Materiales de Madrid, CSIC, Madrid 28049, Spain
[5] Servicio de Cirugía General II, Hospital Marqués de Valdecilla, Santander 39008, Spain

E-mail: slopez@iuma.ulpgc.es

Received 18 April 2006, accepted for publication 7 August 2006
Published 1 September 2006
Online at stacks.iop.org/PM/27/1033

Abstract

Photoplethysmography and pulse oximetry are techniques based on optical principles, which are widely used in medical practice for non-invasive monitoring. There are some processes which may affect specific organs or parts without a significant repercussion on the information provided non-invasively. Here, we report on the preliminary results obtained by transmittance photoplethysmography in pig intra-peritoneal organs along a surgical intervention, using a measurement system based on two near-infrared laser diodes. Analysis of the signals recorded at 750 nm and 850 nm in the mesentery root, mesocolon, gastric wall and aorta artery has shown the affordability of performing *in situ* photoplethysmography for visceral perfusion evaluation.

Keywords: laser diodes, optical sensor, photoplethysmography, viscera

1. Introduction

Photoplethysmography and pulse oximetry are widely used in human clinics as non-invasive techniques to monitor the heart rate and the oxygen saturation of arterial blood haemoglobin. There are some processes which may affect specific organs or parts without significant repercussion on the parameters non-invasively measured from an extremity (finger or toe). Such situations are present in mesentery ischemia or thrombosis, and frequently cause an urgent laparotomy. Direct determination of the perfusion and oxygenation degree in the

intestinal wall and other territories is very useful for more precise diagnostic and therapeutic efficiency.

Several publications have been devoted to the study of techniques based on optical principles for an objective evaluation of visceral perfusion and the viability of intra-peritoneal tissues and organs. These studies have been performed in patients (Ouriel *et al* 1988, Salo *et al* 1992, Garcia-Granero *et al* 1997, Delaney *et al* 1999, La Hei and Shun 2001, Crerar-Gilbert *et al* 2002) and animal models (Whitehill *et al* 1988, Vahl *et al* 1995, Uribe *et al* 1995, Avino *et al* 1995, Koga *et al* 2002), using photoplethysmography (Ouriel *et al* 1988, Whitehill *et al* 1988, Uribe *et al* 1995, Avino *et al* 1995, Garcia-Granero *et al* 1997, Crerar-Gilbert *et al* 2002) and pulse oximetry (Ouriel *et al* 1988, Salo *et al* 1992, Vahl *et al* 1995, Avino *et al* 1995, Yilmaz *et al* 1999, Delaney *et al* 1999, La Hei and Shun 2001, Koga *et al* 2002, Crerar-Gilbert *et al* 2002) in transmission (Ouriel *et al* 1988, Salo *et al* 1992, Avino *et al* 1995) or reflection mode (Vahl *et al* 1995, Garcia-Granero *et al* 1997, Yilmaz *et al* 1999, Koga *et al* 2002, Crerar-Gilbert *et al* 2002).

Despite the positive evidence of the authors regarding the usefulness of photoplethysmography and pulse oximetry, there are some reports which account for certain shortcomings (Whitehill *et al* 1988, Avino *et al* 1995, Delaney *et al* 1999, Koga *et al* 2002). Early authors (Whitehill *et al* 1988) pointed out that the detection threshold of photoplethysmography may be below the minimal flow requirements necessary for tissue viability and that the photoplethysmographic waveform should not be used as a reliable assurance of the ultimate viability of ischemic intestinal tissue. Later, the results of Avino *et al* (1995) supported the findings of other authors (such as Ouriel *et al* 1988) that pulse oximetry can be applied to the intestine and can measure transcolonic oxygen saturation and arterial pulsatility. However, these authors remarked that the usefulness of this technique is limited by its inability to differentiate partial from complete hypoperfusion or from adequate perfusion when the pulsatility of the signal is lost. Afterwards, Delaney *et al* (1999) used a technique similar to that described by Ouriel *et al* (1988), but the pulse oximetry probe did not reproducibly read signals from the colon in 8 of 13 patients even though signals were easily obtained from the small bowel in each case. Their results demonstrated that the use of pulse oximetry was not as easily reproduced as previously suggested. More recently, Koga *et al* (2002) concluded, after a study of 14 piglets with a reflectance probe, that sigmoid colonic endoluminal pulse oximetry may not be a suitable method for monitoring colonic ischemia. Almost at the same time, Crerar-Gilbert *et al* (2002) obtained measurable photoplethysmographic signals from the surface of the bowel (12 patients), the liver (eight patients) and the kidney (six patients), using a purpose-built reflectance probe with peak emissions at 665 nm (red) and 880 nm (infrared). These last authors concluded that their findings indicated the feasibility of reflectance pulse oximetry for measuring the oxygenation of abdominal organs.

Up to the present moment, no technique for intra-cavitary (intra-abdominal/thoracic, endoluminal, endovascular, etc) monitoring has come into routine clinical practice. Therefore, it is still attractive to study new devices, which could improve the available techniques and allow reliable *in situ* measurement of the perfusion and oxygenation degree in several intra-corporeal territories. Here, we report on the the preliminary results derived after analysis of the transmittance photoplethysmographic signals recorded in pig intra-peritoneal organs along a surgical intervention, using a measurement system previously developed (López-Silva *et al* 2003). The aim of the present work is to demonstrate that it is possible to obtain photoplethysmographic signals from different viscera with a sensor based on two near-infrared laser diodes emitting at wavelengths of interest for pulse oximetry.

2. Methods

2.1. Photoplethysmography and pulse oximetry principles

Photoplethysmography is a technique that provides a signal proportional to changes in blood volume (Kamal *et al* 1989). Thus, photoplethysmography is a simple and useful method for measuring the pulsatile component of the heartbeat and evaluating the circulation (Nakajima *et al* 1996). Pulse oximetry (Aoyagi *et al* 1974, Yoshiya *et al* 1980, Yoshiya and Shimada 1983) combines photoplethysmography with differential optical absorption of oxy- (HbO_2) and deoxyhaemoglobin (RHb) at two specific wavelengths to measure the arterial oxygen saturation. This approach assumes that the time-variant photoplethysmographic signal (PPG) is caused solely by changes in the arterial blood volume associated with the cardiac cycle and that no other haemoglobin derivatives different from HbO_2 or RHb are present. Photoplethysmography and pulse oximetry readings can be obtained both from transmitted and reflected signals using sensors with the appropriate configuration. The variable component of the photoplethysmogram results from the expansion and relaxation of the arterial bed, while the constant component is due to the light attenuation by non-pulsatile arterial blood, venous blood and tissue. The wavelengths used in pulse oximetry are typically around 660 nm in the red region and anywhere from 800 to 1000 nm in the near-infrared region (Pologe 1987). Almost all commercial pulse oximeters use light emitting diodes (LEDs) as sources, with emissions near 660 nm, in the red region of the optical spectrum, and in the 880–940 nm infrared (Lindberg *et al* 1995, Mannheimer *et al* 1997).

Oxygen saturation refers, by definition, to that part of the haemoglobin concentration in the blood that can combine reversibly with oxygen (Zijlstra and Oeseburg 1989). Blood does always contain small amounts of haemoglobins that are, through various causes, permanently or temporarily unable to bind oxygen (dyshaemoglobins). The most common dyshaemoglobins are carboxyhaemoglobin and methaemoglobin. Consequently, oxygen saturation is the ratio of the oxyhaemoglobin concentration with respect to the concentration of total haemoglobin, without the dyshaemoglobins.

Oxygen saturation (So_2), as measured by pulse oximetry principles, is obtained by analysing the variable component (E_{AC}) of the PPG, related to the corresponding constant component (E_{DC}) of the PPG, at two specific wavelengths λ_1 and λ_2 (Yoshiya and Shimada 1983). The ratio of these signals at both wavelengths, $\left(E_{AC}^{\lambda 1}/E_{DC}^{\lambda 2}\right)/\left(E_{AC}^{\lambda 1}/E_{DC}^{\lambda 2}\right)$, is representative of the absorption by the arterial blood. Some theoretical equations assume the validity of Beer–Lambert's law for deriving the relationship between the oxygen saturation and the measured optical properties of a pulsating vascular bed through the specific absorption coefficients of RHb and HbO_2. The attenuation of the optical radiation by a vascular bed is not only due to blood RHb and HbO_2 absorption, but also due to multiple scattering in the red blood cells and tissue structures. Thus, from a practical point of view, the real relationship between So_2 and the ratio of the signals is derived from an experimental calibration procedure (Mendelson and Kent 1989). Hence, the presence of a measurable pulsating signal is essential for the successful operation of a pulse oximeter.

2.2. Measurement system

The measurement system previously developed (López-Silva *et al* 2003) is shown in figure 1. It comprises the optical sensor, sensor electronics, data acquisition board (DAQ) and a handheld personal computer (PC). The DAQ and the programs for measurement control, data acquisition and processing are installed in the PC. The configuration of the developed optical sensor

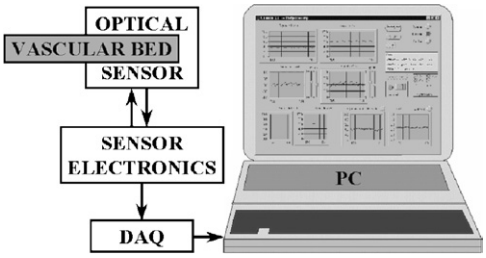

Figure 1. Scheme of the whole measurement system for photoplethysmography and pulse oximetry. The analysed vascular bed is placed between both sides of the transmittance optical sensor. The laser-diode driver, amplification stages, timing and sample-and-hold circuits constitute the sensor electronics. The data acquisition board (DAQ) and the programs are installed on a personal computer (PC).

corresponds to the transmission mode, the emitters and the photo-detectors being situated in opposite sides with respect to the vascular bed analysed.

Two laser diodes with peak wavelengths close to 750 nm and 850 nm are used as optical emitters in the transmittance optical sensor. Figure 2 shows the emission peaks of the laser diodes with respect to the absorption spectra (millimolar absorptivities, l mmol^{-1} cm^{-1}) of adult human haemoglobin derivatives, oxyhaemoglobin and deoxyhaemoglobin (HbO_2 and RHb, respectively, data from Zijlstra *et al* 1991, De Kock 1991) and emission bands of red (660 nm) and infrared (870 nm) LEDs (adapted from López Silva 1997). The laser diode of 750 nm matches a local maximum of the RHb optical absorption, over HbO_2. In 850 nm, the RHb optical absorption is smaller than that of HbO_2. Thus, the near-infrared (NIR) laser diodes (LD) can replace the LEDs of the classical pulse oximeters. In the optical sensor, to reduce the mismatch in the volumes probed by each wavelength and to minimize the movement artefacts, two LD chips are mounted on a single metal heat sink with a separation distance of 0.7 mm between their central parts. Both chips are situated so that their emission beam larger divergence axes are parallel to the sensor central longitudinal axis. Three BPW34 p-i-n silicon photodiodes (PD) are connected in parallel and aligned to increase the photo-detection area. In the PD backside is situated the first amplifier stage, which converts the photocurrent into a proportional voltage. The optical emitters and detectors are mounted in a modified reusable spring-loaded clip pulse oximetry probe.

The laser-diodes driver, amplification stages, timing and sample-and-hold (S&H) circuits constitute the sensor electronics (figure 1). The laser-diodes driver sequentially activates each LD during 5 μs at a repetition rate of 1 kHz. The outputs of the S&H, with independent channels for the signals of each LD, are fed into the analogue inputs of a 12-bit DAQ (DAQ1200, National Instruments). The S&H output signals are analogically pre-filtered by the DAQ with a simple anti-aliasing RC low-pass filter at 300 Hz. After that, the signals are digitized at 1 kSa s^{-1} for every channel. The next stages of the signal processing are carried out digitally, either online (in real time) or offline (post-processing). A ten-sample averaging of each wavelength PPG signal is performed and 100 Sa s^{-1} is stored for optional post-processing.

Each wavelength PPG signal is decomposed into its variable or pulsating component (E_{AC}) and constant or non-pulsating component (E_{DC}), using processing algorithms previously developed (Giannetti *et al* 1998, 2004, López Silva *et al* 2003, Silveira *et al* 2005). Figure 3 exposes the diagrams of two processing algorithms, processing algorithm 1 (PA1) and processing algorithm 2 (PA2), implemented to obtain the heart rate values for each wavelength in a given time interval. The processing algorithms begin with a low-pass Bessel filtering (cut-off frequency f_1, order $n = 6$) in order to obtain the constant value of each flow of the

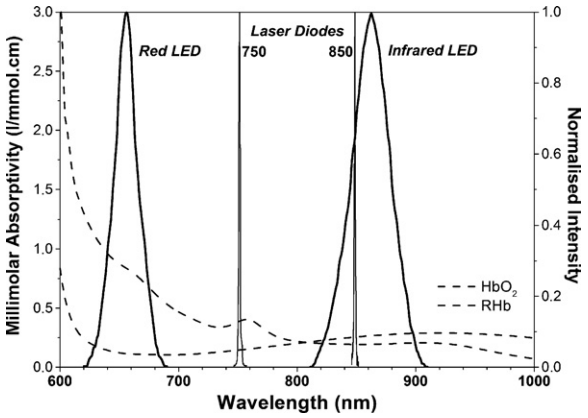

Figure 2. Absorption coefficients of oxyhaemoglobin (HbO_2) and deoxyhaemoglobin (RHb), normalized emission spectra of red and infrared light emitting diodes (LED) and normalized emission spectra of our laser diodes (750 nm and 850 nm).

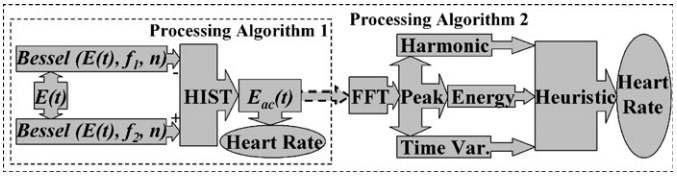

Figure 3. Flow diagram of the processing algorithms.

raw PPG signals $E(t)$. This value is almost constant or non-variable over the period of the variable component of the PPG and is directly suitable to be used as E_{DC}. A second similar Bessel filter with cut-off frequency f_2 is used to suppress high-frequency noise and ripple. The band-pass filtered signal $E_{ac}(t)$ of each flow of raw PPG signals $E(t)$ is then obtained from the difference between the outputs of the two low-pass Bessel filters. We selected the Bessel filter of sixth order because of the higher linearity in phase response offered, which is reflected in a minor distortion in the shape of the PPG signals. After Bessel filtering, nonlinear filtering is performed through the histogram analysis (HIST). The heart rate value in a given time interval is derived from the flow of variable signals $E_{ac}(t)$. The peak-to-peak value of the pulsating component (E_{AC}) can also be derived through a histogram reduction procedure in HIST (Giannetti *et al* 1998, López Silva *et al* 2003).

The second processing algorithm (Giannetti *et al* 2004, Silveira *et al* 2005) adds to the first one a frequency domain-based approach, as shown in figure 3. This approach analyses the variable signals by applying a fast Fourier transformation (FFT) to a moving window of data and extracts from that the information of the harmonic contents of the components of the global photoplethysmographic signal. The power spectra of the signals is analysed by a heuristic approach, which considers the harmonic content, energy and timing variation of the spectra to derive the heart rate.

The algorithms have been implemented using Lab Windows CVI™ facilities so that processing can be carried out both in real time and in offline (post-processing). In the PC monitor are displayed the raw PPG signals, their constant and variable components, and the heart rate values. In a user friendly manner, it is possible to set up the filter parameters and the time processing interval and select the generation of files containing the 100 Sa s^{-1} PPG

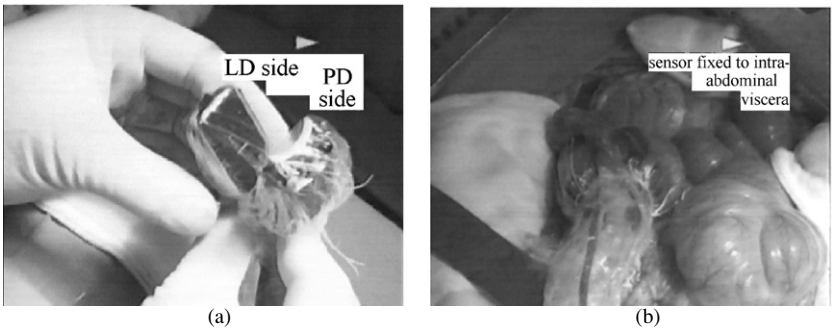

(a) (b)

Figure 4. The near-infrared laser diode-based transmittance optical sensor. View of the laser diode (LD) and the photodiode (PD) sides of the optical sensor (a). The sensor prototype is inserted in a sterile protection plastic and fixed to a pig's intra-abdominal viscera (b).

signals for both wavelengths as well as the results obtained after all the processing. Since the signal pulsation is generated by the beating heart, one can reasonably assume that it will be over 0.5 Hz or 30 beats per minute (bpm) and not exceed 5 Hz, i.e. 300 bpm (Pologe 1987). Because of that, the cut-off frequency values are of the order of some tenths of Hertz for f_1 and in the range of 5–30 Hz for f_2. In the present study, the cut-off frequencies of the Bessel filters (figure 3, left) were set as $f_1 = 0.25$ Hz and $f_2 = 15$ Hz.

2.3. Photoplethysmography in intra-peritoneal organs

The aim of the prospective study was the short time record of transmittance photoplethysmographic signals in viscera, using a sensor with laser diodes emitting in two wavelengths of interest for pulse oximetry. The animal study was conducted in the Laboratory of Experimental Surgery at the Faculty of Medicine of the University of Cantabria (Spain), after approval by the Animal Research Ethical Committee. The study was performed in intra-peritoneal organs of one large white pig with a weight of 16 kg, which was obtained and manipulated according to the Animal Welfare Act ethical statements for research animals. The pig was intramuscularly pre-medicated with 15 mg per kg ketamine and 0.1 mg atropine. Induction of general anaesthesia was performed with 10 mg per kg sodium pentothal, which was injected intravenously. It was followed by endotracheal intubation. Ventilation was performed with 16 breaths per minute. Anaesthesia was maintained after intubation by NO_2 and O_2 breath at 6 l per minute and 0.075 mg per kg fentanyl plus 2 mg per 20–30 min pancuronium bromide administered intravenously. A laparotomy under conventional aseptic conditions permitted to reach the intra-abdominal viscera.

The transmittance sensor was inserted in a sterilized protection plastic (figure 4(a)) and then fixed to specific intra-peritoneal organs, as shown in figure 4(b). The sterile protection plastic (camera cover rolled, MTP Medical Technical Promotion Gmbh, Tuttlingen, Germany) was transparent in the spectral range of the optical emitters. Prior to register the PPG, the operating lights were switched off and the injection current of each laser diode was adjusted to avoid either low signal levels or detector saturation. The injection current was higher than the threshold current (I_{th}) with injection values between 1.5 I_{th} and 2.5 I_{th}. The injection currents of the laser diodes, as a factor of the threshold current, were 1.56 I_{th1} (in the gastric wall), and 1.65 I_{th1} (in the mesocolon, mesentery root and aorta artery) for LD1 (750 nm), and 2.15 I_{th2} (in the gastric wall), 2.35 I_{th2} (in the mesocolon and mesentery root) and 2.42 I_{th2} (in the aorta artery) for LD2 (850 nm). The sensor was kept in place until stable photoplethysmographic

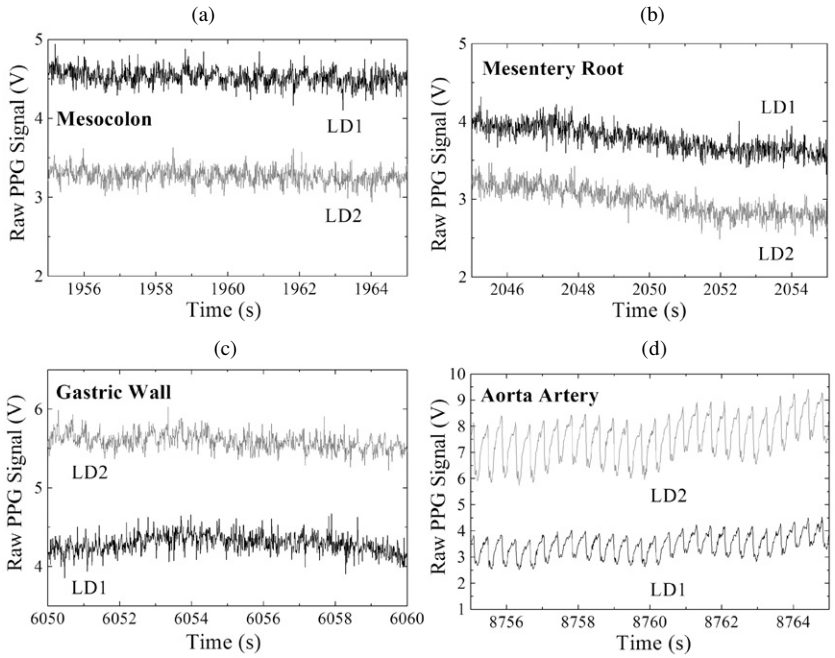

Figure 5. Raw transmittance photoplethysmographic (PPG) signals recorded over 10 s intervals in the pig mesocolon (a), mesentery root (b), gastric wall (c) and aorta artery (d), using the laser diodes (LD1 and LD2).

signals were achieved. Special care was taken to avoid the excessive compression of the tissues, which could affect the blood perfusion. Two-wavelength PPG signals (LD1—750 nm and LD2—850 nm) were recorded in the mesocolon, mesentery root, gastric wall and aorta artery. Electrocardiography (ECG) and arterial pressure were continuously monitored, their values being 150 beats per minute and 120/90 respectively over the whole experiment. At the conclusion of the experiment, the pig was sacrificed with KCl intravenously and ventricular fibrillation.

3. Results

Figure 5 presents the raw PPG recorded with LD1 (750 nm) and LD2 (850 nm) in 10 s intervals in the mesocolon (a), mesentery root (b), gastric wall (c) and aorta artery (d). FFT analysis using a Hanning window was performed in 10 s time intervals of the raw PPG signals in every 5 s, over 60 s in the mesocolon (figures 6(a) and (b)), gastric wall (figures 6(e) and (f)) and aorta artery (figures 6(g) and (h)), and over 15 s in the mesentery root (figures 6(c) and (d)). The values shown in the time interval axis in figure 6 correspond to the last time value of each 10 s time interval. Thus, for instance, 1930 s (time interval axis in figure 6(a)) is the last time value of the time interval from 1920 s to 1930 s. The FFT analysis has shown, for both laser diodes, LD1 (750 nm in figures 6(a), (c), (e) and (g)) and LD2 (850 nm in figures 6(b), (d), (f) and (h)), a clear peak frequency around 2.5 Hz in all of the studied organs (aorta artery, mesocolon, mesentery root and gastric wall). Despite the differences in the raw PPG, this peak frequency is in coincidence with the 150 bpm of the ECG record. A similar FFT analysis was performed using a Hamming window with identical results in all of the organs and LDs.

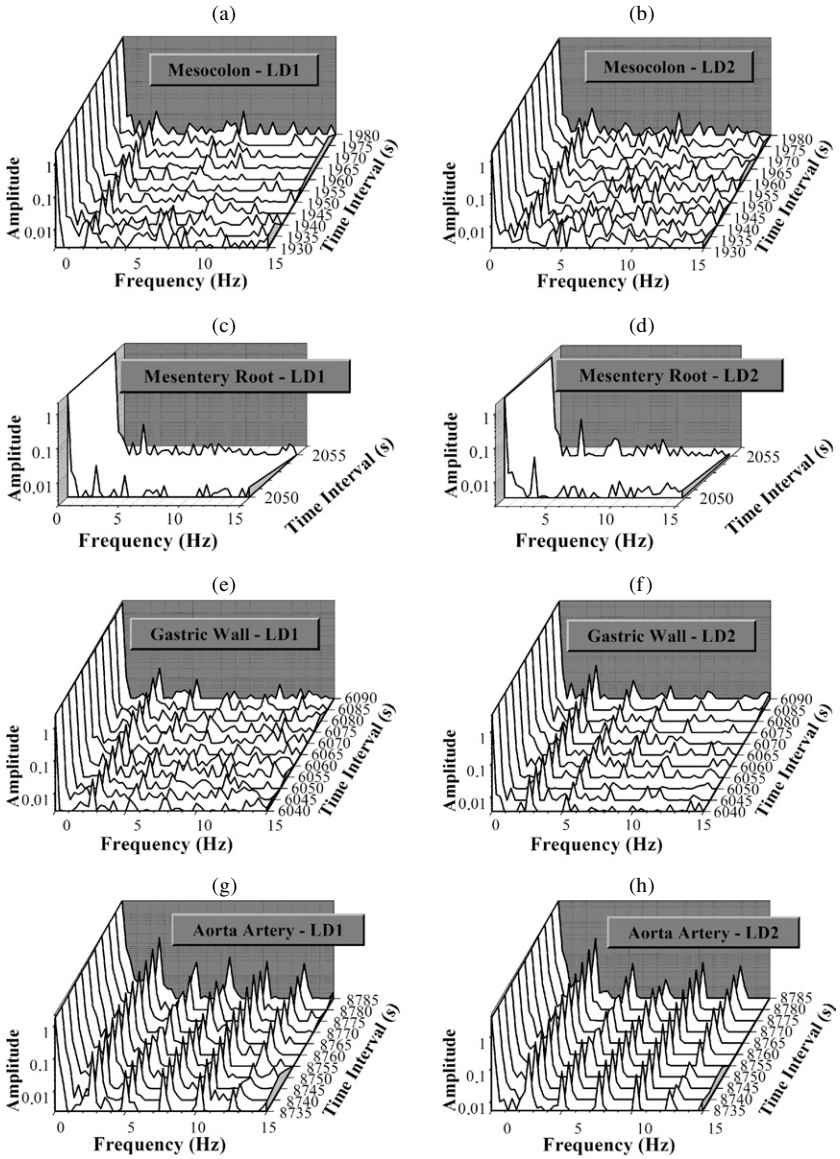

Figure 6. FFT analysis of the raw transmittance photoplethysmographic signals recorded over 10 s time intervals in every 5 s in a pig's mesocolon (a), (b), mesentery root (c), (d), gastric wall (e), (f) and aorta artery (g), (h), using the laser diodes (LD1 and LD2).

Figure 7 shows the raw PPG recorded with LD1 (750 nm) and LD2 (850 nm) over 60 s intervals in the mesocolon (a), mesenteric root (c), gastric wall (e) and aorta artery (g) and the corresponding pulsation rates (beats per minute, bpm in figures 7(b), (d), (f) and (g)), obtained by the processing algorithms 1 and 2, as shown in figure 3 (PA1 and PA2, respectively, in figures 7(b), (d), (f) and (h)). The processing with the algorithm 1 (figure 3, left) was performed online (in real time, along the experiment), and the pulsations were obtained for PPG signals from LD1 (750 nm). The processing with the algorithm 2 (whole figure 3) was performed offline (post-processing after the experiment), and the pulsations were obtained

Table 1. Mean values and standard deviations of the pulsation rates derived using the second processing algorithm in the intra-peritoneal organs.

Intra-peritoneal organ	Emitter	Time interval (s)	Mean (bpm)	SD (bpm)	n
Mesocolon	LD1	1920–1980	138.8	25.5	24
Mesocolon	LD 2	1920–1980	139.5	22.8	24
Mesocolon	LD 1	1920–1975	146.2	1.2	22
Mesocolon	LD 2	1920–1975	146.0	1.7	22
Mesentery root	LD1	2040–2055	124.5	33.9	6
Mesentery root	LD2	2040–2055	137.7	0.0	6
Gastric wall	LD1	5970–6090	155.4	3.0	46
Gastric wall	LD2	5970–6090	155.2	2.9	46
Aorta artery	LD1	8725–8785	153.6	1.5	23
Aorta artery	LD2	8725–8785	153.6	1.5	23

from both LD1 (750 nm) and LD2 (850 nm). The results correspond to processing performed every 2 s in time intervals of 10 s.

Table 1 gives the mean values (mean), the standard deviations (SD) and the number of points (n) of the pulsation rates derived using the second processing algorithm (PA2 in figures 3 and 7), from each intra-peritoneal organ and for both optical emitters (LD1 and LD2), at the time intervals displayed in figures 7(b), (d), (f) and (g). The statistics for mesocolon have been calculated both considering all the points of the time interval ($n = 24$, 1920–1980 s)and excluding the last two results from that interval ($n = 22$, indeed, 1920–1975 s).

4. Discussion

The raw photoplethysmographic signals recorded with LD1 (750 nm) and LD2 (850 nm) in 10 s intervals in the aorta (figure 5(d)) differ from those corresponding to the mesocolon (figure 5(a)), mesentery root (figure 5(b)) and gastric wall (figure 5(c)). The aorta artery signals have large peak-to-peak pulsating components with few spikes in comparison to those signals from the mesocolon, mesentery root and gastric wall. The E_{AC} to E_{DC} ratios are around 30% for the aorta artery and below 15% for the other three organs, respectively. The fact that there is a gradient in the amplitude of the pulsating component from the aorta to the gastric wall, mesocolon and mesentery root, can be attributed to the physiological decrease in pressure as we move further from the heart. Despite these differences, the FFT analysis of the raw PPG performed in diverse 10 s intervals (figure 6) has shown a clear peak frequency around 2.5 Hz in all of the cases for both LD1 and LD2. This frequency value would correspond to 150 pulsations or beats per minute, which is in coincidence with the heart rate values of the ECG monitorization.

Additional oscillations are observed in the PPG of the aorta artery (figures 5(d) and 7(e)) and gastric wall (figure 7(c)) over the whole time intervals. The FFT analysis of the aorta artery signals in 10 s and 30 s intervals has shown a peak frequency around 0.3 Hz. These aorta artery oscillations seem to be related to respiratory rate since the ventilation rate was 16 breaths per minute (around 0.27 Hz). The oscillations in the gastric wall PPG are slightly higher than 3 beats per minute and could be associated with observed peristaltic movements.

The pulsation rates derived online for one laser diode using the first processing algorithm in the aorta artery (PA1-LD1 in figure 7(h)) agree with the heart rate obtained by ECG (150 beats per minute), although some points are out of this behaviour pattern. The rates obtained with LD1 using PA1 in the mesocolon, mesentery root and gastric wall (PA1-LD1 in

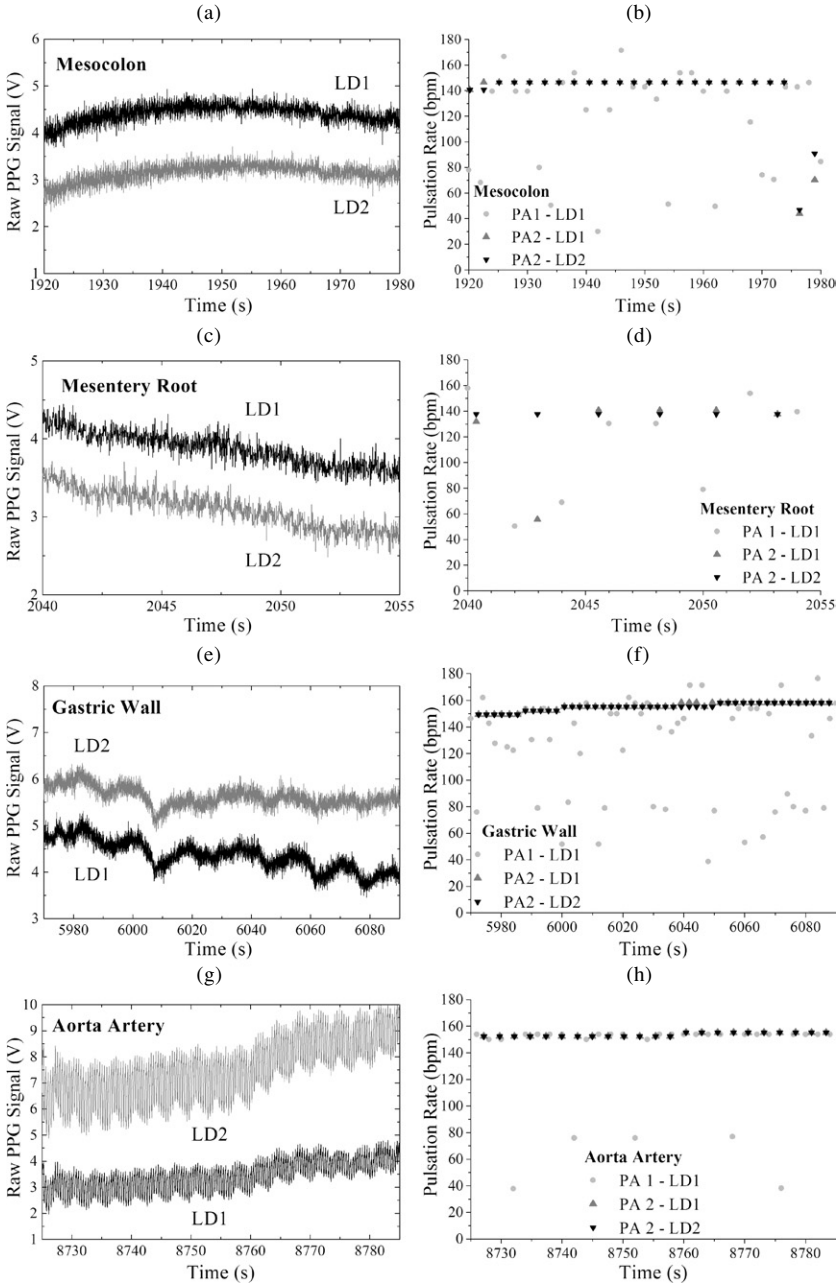

Figure 7. Pulsation rate values (beats per minute (bpm) in (b), (d), (f), (h)) obtained through two processing algorithms (PA1, PA2) of the raw photoplethysmographic signals (PPG in (a), (c), (e), (f)), in a pig's mesocolon (a), (b), mesenteric root (c), (d), gastric wall (e), (f) and aorta artery (g), (h), using the transmittance sensor based on two laser diodes (LD1, LD2).

figures 7(b), (d) and (f), respectively) substantially differ from the 150 beats per minute. Similar results have been obtained offline for the second laser diode (LD2) in all of the organs using the first processing algorithm (PA1). The pulsation rates derived offline for

both laser diodes with the second processing algorithm in the mesocolon, mesentery root, gastric wall and aorta artery (PA2-LD1 and PA2-LD2, in figures 7(b), (d), (f) and (h)) show a good agreement with the ECG value and are stable over the whole time intervals. The oscillations observed in the PPG signals of the gastric wall and the aorta artery (figures 7(e) and (g)) do not affect the pulsation rates obtained with the second processing algorithm (PA2 in figures 7(f) and (h)). In order to obtain the pulsation rates, it has been necessary to discriminate the cardiac pumping-related signals from movement artefacts (such as peristaltic movements and respiration) through a more complex processing.

As may be seen from the mean values and SD in table 1, there is small variability among the pulsation rates derived in all the intra-peritoneal organs using the PA2. Although the time intervals range from 15 s to 120 s (2 min), the pulsation rate values are repeatable. At the beginning of the experimental study (1920–1975 s), the pulsations in the mesocolon are about 146 bpm. 1 h later (5970–6090 s), the rates in the gastric wall are near 155 bpm. Finally, almost 2 h after the measurement in the mesocolon and about 45 min after the measurement in the gastric wall, the values for the aorta artery (8725–8785 s) are around 154 bpm. These quantitative results are within an acceptable 4% of error and may also reflect small physiological oscillations around 150 beats per minute. Therefore, the second processing algorithm allows us to obtain reliable pulsation values from the photoplethysmographic signals recorded in all of the studied organs using both laser diodes.

The objective of this preliminary study has been to prove the short time record of photoplethysmographic signals in some intra-peritoneal territories, using a sensor based on two near-infrared laser diodes with emissions in wavelengths of interest for pulse oximetry. The analysis and post-processing of these photoplethysmographic signals have let to quantify the time changes in the blood volume, as indicative of the visceral perfusion, which constitute the first step towards the implementation of pulse oximetry. To our knowledge, no experimental works have been addressed to the simultaneous application of different far-red or near-infrared wavelengths to intra-peritoneal monitoring.

Our wavelength selection is justified by promising technical facts and issues. For the lower oxygen saturation, numerical modelling (Mannheimer *et al* 1997) has suggested that significantly better accuracy can be expected when a far-red (such as 735 nm) and a near-infrared emitter pair are used, which has been applied to sensors for foetal monitoring (Reuss 2004). Another advantage of NIR wavelengths is the deeper penetration of the optical radiation (Jöbsis 1977), which makes it a candidate for an improved sensor to measure in pulsating beds optically denser than normal fingertips (López Silva *et al* 2003). From the point of view of the detection capabilities of the silicon photodiodes, the 750 nm band corresponds to higher values compared with 630–660 nm wavelengths and on the order of 850 nm, being of the same order of the detected photocurrents. The carboxyhaemoglobin absorptivity in the near-infrared range is smaller than the absorptivities of both oxyhaemoglobin and desoxyhaemoglobin (Zijlstra *et al* 1991). Indeed, less interference of the carboxyhaemoglobin on the pulse oximetry reading is expected at the 750–850 nm wavelengths, in comparison with the red range. Our wavelength selection has been ensured through the use of laser diodes in our sensor. Nevertheless, the use of available far-red and near-infrared LEDs with emissions in different wavelengths below and above 800 nm could also serve our purpose.

In the present study we used a transmittance finger probe placed in a sterile transparent plastic bag, which was positioned at each organ at the time of the measurement only. In order to increase the quality of the detected signal, we must improve the attachment of the sensor to the intra-peritoneal organ. It must keep the sensor in a fixed position and avoid the displacement of the analysed tissue or organ with respect to the light emitters and detector, thus minimizing movement artefacts and false readings. In addition, the light from the emitters

should reach the photodetector after passing through the vascular bed, the optical path lengths and probed volumes being as similar as possible for all the emitters. At the same time, the probe must prevent the compression of the tissue since this may result in reduced blood flow and oxygenation. Another alternative to be evaluated is the use of reflectance sensors, in particular using the above-mentioned far-red or near-infrared wavelengths. Therefore, the probe must be modified in size, geometry and ergonomics to be optimally positioned in each organ and to improve the PPG characteristics.

The differences in the PPG signals of each organ, at both wavelengths, show the differences in the optical response of each tissue (tissue composition and structure, thickness, haemoglobin content). This fact is very important if we want to quantify the oxygen saturation of the tissues since the signal levels at both wavelengths should be associated with the oxygenation degree of the studied organs. Because of this, a detailed study must be performed in each tissue.

5. Conclusions

The results presented here demonstrate the feasibility of transmittance photoplethysmography with laser diodes emitting at specific near-infrared wavelengths of interest for pulse oximetry in different intra-peritoneal organs with pulsating vascular beds. The derived pulsation rates are in agreement with the reference heart rate values obtained by electrocardiography. The analysis of the signals recorded at 750 nm and 850 nm in the mesentery root, mesocolon, gastric wall and aorta artery has shown the affordability to perform *in situ* photoplethysmography for visceral perfusion evaluation.

Additional investigations during variable conditions of perfusion and oxygenation are also necessary to demonstrate that this technique may reliably discriminate between normal and abnormal situations in specific intra-peritoneal organs and tissues. Further studies are necessary in order to improve the signal detection, assess the sensor processing algorithms and optimize its parameters for real-time monitoring. This should be accompanied by a calibration study on each tissue, which allows us to obtain the corresponding levels of oxygen saturation from the variable and constant components of the photoplethysmographic signal.

Acknowledgments

The authors gratefully acknowledge the assistance of Dr J M García in revising the present manuscript. This work has been partially supported by the Spanish Commission for Science and Technology (CICYT) project TIC98–1025, Asociación Cántabra de Cirugía, project UNI 2002/15 of University of Las Palmas de Gran Canaria and grant FIS PI040715 of Spanish Ministry of Health. Spanish Programa Ramón y Cajal supports SMLS.

References

Aoyagi T, Kishi M, Yamaguchi K and Watanabe S 1974 Improvement of an earpiece oximeter *Abstracts of the Japanese Society of Medical Electronics and Biological Engineering (Tokyo, Japan)* pp 90–1

Avino A J, Oldenburg W A, Gloviczki P, Miller V M, Burgart L J and Atkinson E J 1995 Inferior mesenteric venous sampling to detect colonic ischemia: a comparison with laser Doppler flowmetry and photoplethysmography *J. Vasc. Surg.* **22** 271–7

Crerar-Gilbert A J, Kyriacou P A, Jones D P and Langford R M 2002 Assessment of photoplethysmographic signals for the determination of splanchnic oxygen saturation in humans *Anaesthesia* **57** 442–5

De Kock J P 1991 Pulse oximetry: theoretical and experimental models *DPhil Dissertation* University of Oxford

Delaney C P, Couse N F, Mehigan D and Keaveny T V 1999 Inferior mesenteric venous sampling, pulse oximetry, and assessment of colonic perfusion during aortic aneurysm surgery *Dig. Dis. Sci.* **44** 1786–91

Garcia-Granero E, Alos R, Uribe N, Sala C and Lledo S 1997 Intraoperative photoplethysmographic diagnosis of ischemic colitis *Am. Surg.* **63** 765–8

Giannetti R, López Silva S M, Dotor M L, Sendra J R, Silveira J P and Briones F 1998 An innovative signal processing algorithm for near infrared laser-based pulse oximeter *Proc. IMEKO TC-4* pp 153–6

Giannetti R, Silveira J P, Dotor M L, Golmayo D, Martín P, Miguel-Tobal F, Bilbao A and López-Silva S M 2004 Oxygen saturation measurements in athletes attaining maximal exertion conditions *Proc. 21st IEEE/IMTC* vol 1 pp 740–4

Jöbsis F F 1977 Noninvasive, infrared monitoring of cerebral and myocardial oxygen sufficiency and circulatory parameters *Science* **198** 1264–7

Kamal A A R, Harness J B, Irving G and Mearns A J 1989 Skin photoplethysmography—a review *Comp. Methods Programs Biomed.* **28** 257–69

Koga I, Stiernström H and Wiklund L 2002 Sigmoid colonic reflectance pulse oximetry and tonometry in a porcine experimental hypoperfusion shock model *Acta Anaesthesiol. Scand.* **46** 1212–6

La Hei E R and Shun A 2001 Intra-operative pulse oximetry can help determine intestinal viability *Pediatr. Surg. Int.* **17** 120–1

Lindberg L G, Lennmarken C and Vegfors M 1995 Pulse oximetry—clinical implications and recent technical developments *Acta Anesthesiol. Scand.* **39** 279–87

López Silva S M 1997 Oximetría de pulso con diodos láser infrarrojos *Tesis Doctoral* Universidad Complutense de Madrid

López Silva S M, Dotor M L and Silveira J P 2003 NIR transmittance pulse oximetry with laser diodes *J. Biomed. Opt.* **8** 525–33

Mannheimer P D, Casciani J R, Fein M E and Nierlich S L 1997 Wavelength selection for low-saturation pulse oximetry *IEEE Trans. Biomed. Eng.* **44** 148–58

Mendelson Y and Kent J C 1989 Variations in optical absorption spectra of adult and fetal hemoglobin and its effects on pulse oximetry *IEEE Trans. Biomed. Eng.* **36** 844–8

Nakajima K, Tamura T and Miike H 1996 Monitoring of heart and respiratory rates by photoplethysmography using a digital filtering technique *Med. Eng. Phys.* **18** 365–72

Ouriel K, Fiore W M and Geary J E 1988 Detection of occult colonic ischemia during aortic procedures: use of an intraoperative photoplethysmographic technique *J. Vasc. Surg.* **7** 5–9

Pologe J A 1987 Pulse oximetry: technical aspects of machine design *Int. Anesthesiol. Clin.* **25** 137–53

Reuss J L 2004 Factors influencing fetal pulse oximetry performance *J. Clin. Monit.* **18** 13–24

Salo J A, Perhoniemi V J, Heikkinen L O, Verkkala K A and Järvinen A A 1992 Pulse oximetry for the assessment of gastric tube circulation in esophageal replacements *Am. J. Surg.* **163** 446–7

Silveira M J P, Dotor C M L, Golmayo F M D, Bilbao M A, Giannetti R, López S S M, Martín E P and Miguel T F 2005 Método para procesar señales fotopletismográficas obtenidas de una persona o animal, y oxímetro que utiliza dicho método *Patent* ES200501425

Uribe N, Garcia-Granero E, Belda J, Calvete J, Alos R, Marti F, Gallen T and Lledo S 1995 Evaluation of residual vascularisation in oesophageal substitution gastroplasty by surface oximetry-capnography and photoplethysmography. An experimental study *Eur. J. Surg.* **161** 569–73

Vahl A C, Van Rij G L, Visser J J, Nauta S H M, Vink G Q M, Scheffer G J, de Lange de Klerk E S M, Uyterlinde A, Brom H L F and Rauwerda J A 1995 Endoluminal pulse oximetry in schemic colon in a swine model *J. Am. Coll. Surg.* **180** 57–64

Whitehill T A, Pearce W H, Rosales C, Yano T, Van Way C W and Rutherford R B 1988 Detection thresholds of nonocclusive intestinal hypoperfusion by Doppler ultrasound, photoplethysmography, and fluorescein *J. Vasc. Surg.* **8** 28–32

Yilmaz E N, Vahl A C, van Rij G, Nauta S H, Brom H L and Rauwerda J A 1999 Endoluminal pulse oximetry of the sigmoid colon and the monitoring of the colonic circulation *Cardiovasc. Surg.* **7** 704–9

Yoshiya I, Shimada Y and Tanaka K 1980 Spectrophotometric monitoring of arterial oxygen saturation in the fingertip *Med. Biol. Eng. Comp.* **18** 27–32

Yoshiya I and Shimada Y 1983 Non-invasive spectrophotometric estimation of arterial oxygen saturation *Noninvasive Physiological Measurements* (New York: Academic) pp 251–86

Zijlstra W G and Oeseburg B 1989 Definition and notation of hemoglobin oxygen saturation *IEEE Trans. Biomed. Eng.* **36** 872

Zijlstra W G, Buursma A and Meeuwsen van der Roest W P 1991 Absorption spectra of human fetal and adult oxyhemoglobin, deoxyhemoglobin, carboxyhemoglobin and methemoglobin *Clin. Chem.* **37** 1633–8